Nanoindentation Technique Approach to Predict the Surface-Coating Endurance on Articular Cartilage

Boonyong Punantapong[1*,2], Somchai Thongtem[1], Michael J. Fagan[3] and Chairoj Soorapanth[4]

[1] *Faculty of Science, Chiang Mai University, Chiang Mai 50200, Thailand*

[2] *Faculty of Applied Science, King Mongkut's Institute of Technology North Bangkok, Bangkok 10800, Thailand*

[3] *Centre for Medical Engineering and Technology, University of Hull, Hull, UK*

[4] *Department of Orthopedic Surgical, Bangkok Metropolitan Administration Medical College and Vajira Hospital, Bangkok 10300, Thailand*

**Corresponding author. E-mail: bpp@kmitnb.ac.th*

ABSTRACT

In the case of surface-coatings application, it is crucial to establish when the substrate is reached to prevent catastrophic consequences. Nevertheless, some studies of surface coating have been explained by a coating phenomenon observed below a critical residual coating thickness. The objective of this study was to test the frictional response of the coated articular cartilage to interstitial fluid pressurization which accounts for the osmotic pressure in cartilage by using indentation under dynamic loading. In this study, a model was based on the theory of mixtures for soft hydrated charged tissues, local dissipated energy and related to the friction process under the action of an applied cyclical stress in confined compression over a range of loading frequencies. The experimental results demonstrated that pressurization does take place with increasing loading frequency, concurrently with a decrease in tissue compliance. Therefore, the cartilage dynamic stiffness can be demonstrated experimentally the significance of cartilage deformation as the mechanism of cartilage load support over a wide range of frequency.

Key words: Nanoindentation, Articular cartilage, Surface coating

INTRODUCTION

Articular cartilage is a hydrated soft tissue which serves as the bearing material of diarthrodial joints. It is often highly anisotropic elastically and this needs to be taken into account when analyzing experimental results in elastic properties. The mechanical response of cartilage has been investigated in many studies and it is generally accepted that its viscoelastic response is primarily contributed by the resistive drag of interstitial fluid flowing through the low-permeability collagen-proteoglycan matrix. So the porous structure models have been proposed which describe this mechanical response under various loading conditions and contributes to the load support across the tissue (Gray et al., 1988; Ateshian et al., 1998).

At the same time, theoretical porous media analyses have demonstrated that fluid pressurization contributed to supporting upwards of 90% of the applied stress during contact of cartilage layers (Mow et al., 1980; Fridrici et al., 2003). These studies have suggested that loading situations where contact tractions can be typically as high as 12 MPa, the fluid pressure could act to shield the solid matrix of collagen by maintaining the effective collagen

matrix stress at the level of, e.g., 1.2 MPa. Therefore, the implications of this mechanism are significant in the degradation of cartilage (Oloyede and Broom, 1991; Macirowski et al., 1994).

However, surface coatings are classically used in industrial applications to reduce friction and wear (Fouvry et al., 2003), but it has been a novel in clinical, especially in the biotribological of joints. The coating is usually selected on a trial-and-error basis, which is time-consuming and expensive. That is why laboratory tests and simulated models have been developed to quickly pre-select coating palliatives on articular cartilage. Moreover, the variable of mechanical properties such as thickness, hardness and elastic modulus of coating are very important to evaluate the interactions and lifetime of adhesive in coated articular surface. The aim of this study is to show a method for predictions of the surface coating endurance on articular cartilage, using nanoindentation technique as in an axisymmetric model and analysis by finite element technique.

MATERIALS AND METHODS

For the experimental data acquisition, we used the contact configuration in Figure 1. A biphasic cartilage layer of axisymmetric model of uniform thickness, b is supported by a rigid impermeable subchondral bone substrate. The impermeable indenter contacted the biphasic layer under and applied load intensity, *W* (load per unit length along the out-of-plane or z-direction). So, the indenter is a parabolic approximation to a cylinder of radius, *R*, with a centrally-located sinusoidal ripple of peak-to-peak amplitude, α and wavelength, λ. Then the mathematical representations of the articular layers of the patella, femur and tibia of knee joints are generated from MR imagines. Figure 1 shows a typical set of knee cartilage surfaces, generated using stereophotogrammetric, each grid intersection point on that figure represents a measurement point for that technique. These data were converted to CAD files for analysis by finite element program as ANSYS code (Punantapong et al., 2005).

For the model formulation, the general deviation of the governing equations for a porous deformable layer or charged hydrated soft tissues containing multi-electrolytes is given by Gu et al., (1998). The model employed has assumptions that each phase of the mixture (solid matrix, water, cations and anions) is intrinsically- incompressible solid phase due to fluid exudation from the porous solid matrix, and that the mixture is saturated (Mow et al., 1980). Thus the biphasic theory models cartilage as a mixture of an intrinsically-incompressible solid phase was representing the collagen-proteoglycan-chondrocyte matrix and an intrinsically-incompressible fluid phase was representing interstitial water. Overall tissue compressibility results from fluid transport into or out of the porous-permeable solid matrix. The dissipative drag exerted by the fluid flowing relative to the low-permeability solid matrix imparts a viscoelastic response to the tissue. The general equations of the biphasic theory can be found elsewhere (Mak, 1986; Suh et al., 1995; Gu et al., 1998). Then the reduction of those general equations for the configuration of confined compression has also been described previously (Mow et al., 1980; Sah et al., 1989; Setton et al.,1993; Vlassak and Nix, 1994; Swadener and Pharr, 2001; Fouvry et al., 2003) and is summarized below. Therefore, the governing equations for the mixture is given by

$$\nabla . (\phi^s v^s + \phi^f v^f) = 0 \qquad (1)$$

where $\phi^s + \phi^f$ are the solid and fluid phase velocities, respectively

ϕ^s , ϕ^f are the solid and fluid contents; for a saturated mixture, $\phi^s + \phi^f = 1$

If the balance of linear momentum for each phase, and under quasi-static conditions, the momentum equation for the solid and fluid phases of the tissue are given by

$$\nabla \sigma^{s} + \pi = 0 \tag{2.1}$$

$$\nabla \sigma^{f} - \pi = 0 \tag{2.2}$$

Where σ^{s}, σ^{f} are the solid and fluid stress tensors

π is the momentum exchange between phases due to friction, as fluid particles flows pass the solid phase. In articular cartilage, it has been shown that this term is much more significant than the frictional dissipation between fluid particles (i.e., viscocity) which gives rise to viscous stresses within the fluid.

Hence, volume changes in the tissue result from fluid exudation from the porous solid matrix (Holmes and Mow, 1990). The constitutive relations for the solid and fluid stresses are

$$\sigma^{s} = -\phi^{s} p\mathbf{I} + \lambda_{s} tr(\varepsilon)\,\mathbf{I} + 2\mu_{s}\,\varepsilon \tag{3.1}$$

$$\sigma^{f} = -\phi^{f} p\mathbf{I} + \lambda_{f} tr(\mathbf{D})\,\mathbf{I} + 2\mu_{f}\,\mathbf{D} \tag{3.2}$$

$$\pi = \mathbf{K}(\mathbf{v}^{f} - \mathbf{v}^{s}) + p\nabla\phi^{s} \tag{3.3}$$

where p is the pressure

$\mathbf{I}$ is the identity tensor

$\varepsilon = \frac{1}{2}\left[(\nabla u) + (\nabla u)^{T}\right]$ is the strain tensor for the solid phase

$D = \frac{1}{2}\left[(\nabla v^{f}) + (\nabla v^{f})^{T}\right]$ is the rate of deformation tensor for the fluid phase

$\lambda_{s}\,\mu_{s}$ are the properties of the solid phase, which given by the apparent Lame' constants

$\lambda_{f}\,\mu_{f}$ are the properties of the fluid phase, which given by the apparent first and second viscosity coefficients

$K = (\phi^{f})^{2} / k$, where k is the hydraulic permeability of the porous material (Mow et al., 1980)

Therefore, the total stress is given by (Ateshian et al., 1998)

$$\sigma = \sigma^{s} + \sigma^{f} = -p\mathbf{I} + \lambda_{s} tr(\varepsilon)\,\mathbf{I} + 2\mu_{s}\,\varepsilon + \lambda_{f} tr(\mathbf{D})\,\mathbf{I} + 2\mu_{f}\,\mathbf{D} \cong -p\mathbf{I} + \sigma^{e} \tag{4}$$

where σ^{e} is the effective stress of the solid matrix = $\frac{1}{2} H_{A0}\left(\frac{\lambda^{2}-1}{\lambda^{2\beta+1}}\right) e^{\beta(\lambda^{2}-1)}$, and H_{A0} represents the aggregate modulus under zero strain

At the same time, the experiment of Gu et al., (1998) and Swadener and Pharr, (2001) found that if the solid phase velocity, $\boldsymbol{v}^{s}$ is related to the solid phase displacement $\mathbf{u}$ by the material derivative with respect to the solid phase, $\mathbf{v}^{s} = D^{s}\mathbf{u} / Dt = (\partial \mathbf{u} / \partial t) + (\nabla u)\mathbf{v}^{s}$. Substitution of these constitutive relations into the balance of linear momentum equation in the absence of external body forces, and neglecting inertia forces then:

$$-\phi^s \nabla p + (\lambda_s + \mu_s)\,\nabla\,(\mathrm{div}\mathbf{u}) + \mu_s\,\nabla^2\mathbf{u} + \frac{(\phi^f)^2}{k}\,(\mathbf{v}^f - \mathbf{v}^s) = 0 \tag{5}$$

$$-\phi^f \nabla p + (\lambda_f + \mu_f)\,\nabla\,(\mathrm{div}\mathbf{v}^f) + \mu_f\,\nabla^2\mathbf{v}^f - \frac{(\phi^f)^2}{k}\,(\mathbf{v}^f - \mathbf{v}^s) = 0 \tag{6}$$

It is convenient to define the flux of the fluid relative to the solid phase as

$$\mathbf{w} = \phi^f\,(\mathbf{v}^f - \mathbf{v}^s) \tag{7}$$

for articular cartilage, ϕ^s, ϕ^f ~1; λ_s , μ_s ~10^6Pa; k ~10^{-15} m^4/Ns; λ_f , μ_f ~10^{-3} Pa; and the thickness of cartilage layer ~ 10^{-3} m. Thus, it can be concluded that the term $(\lambda_f + \mu_f)$ ∇ (div$\mathbf{v}^f$) + μ_f $\nabla^2\mathbf{v}^2$ can be neglected in Equation (6). So, Equations (5) and (6) can be rearranged as:

$$-\nabla p + (\lambda_s+\mu_s)\,\nabla\,(\mathrm{div}\mathbf{u}) + \mu_s\,\nabla^2\mathbf{u} = 0 \tag{8}$$

$$\mathbf{w} = -k\nabla p \tag{9}$$

Both of these equations, along with Equation (1), which can be rewritten as div ($\mathbf{v}^2$ + $\mathbf{w}$) = 0 . So, they can be used to solve the dependent variables **u**, **w**, and p subjected to the appropriate boundary conditions.

RESULTS AND DISCUSSION

The computer model was constructed using all of the measured geometric data reported (Ateshian et al., 1998; Punantapong et al., 2005). The finite element analysis meshes for the nanoindentation configuration were created using PRO/Engineer code. The indenter tip was a flat-faced right circular cylinder, aligned perpendicular to the specimen surface; hence the problem could be reduced to an axisymmetric model as shown in Figure 1.

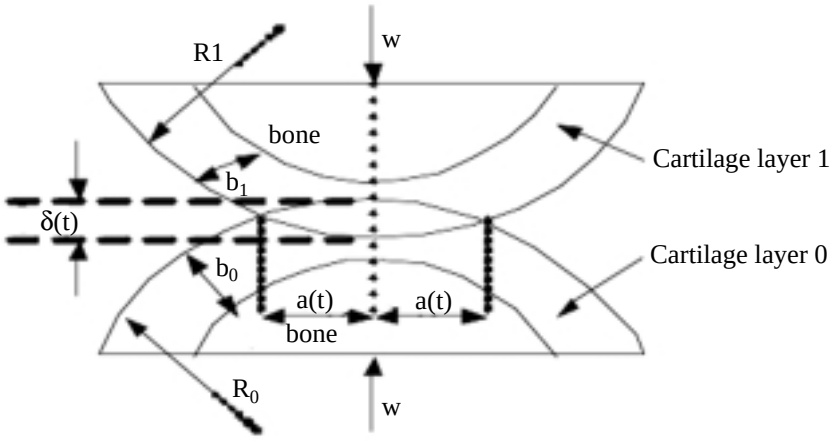

Figure 1. Geometry of the contact configuration for an impermeable indenter on a biphasic surface.

In this study, we used four nodes, axisymmetric elements were used to model the specimen half-space (coating and substrate). The indenter was assumed to be rigid and non-deforming, but it can be translated or rotated as rigid bodies. They also save computing time

since the only variables associated with a rigid surface are translations and rotations on a single node, known as the rigid body reference node. Contact between the rigid indenter surface and the specimen was modeled, using rigid surface contact elements. In the present study, the friction coefficient was set to zero.

The experimental measurements for nanoindentation of articular cartilage coatings estimated that this model was assumed to be constrained at the interface by the soft substrate. The shear stress at the interface was calculated, using a modified version of an analysis by Mow et al., (1980) and Fridrici et al., (2003). The interfacial shear stress increased with applied nano-indenter load as a result of the constraint imposed by the substrate on the coating material, as the polymer is forced away from the indenter axis in the radial direction. Then the critical shear stress was defined by Fouvry et al., (2003).

$$\tau_c = \frac{(P_c - \sigma_y)\,\pi\,(h_f - h_c)}{4(a+\xi)} \tag{10}$$

where P_c is the applied axial stress at the point of interface failure, σ_y is the polymer yield stress, h_f and h_c is the coating thickness under the indenter at the point of interface failure and before the test begins, respectively, a is the radius of the nano-indenter tip and $\xi = 0.55a$ is a material-dependent parameter related to the radial extent of the heavily-deformed coating.

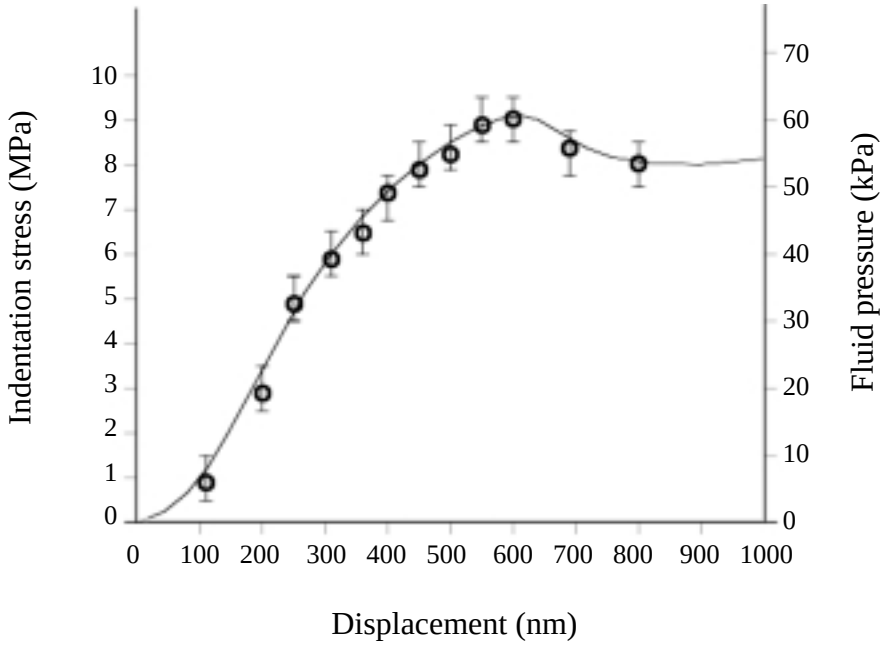

Figure 2. Stress-displacement curve for nanoindentation on an axisymmetric model as coated articular cartilage.

Figure 2 shows the nanoindentation stress-displacement curve on an axisymmetric model as coated articular cartilage using ANSYS code. Prior to interface failure, the nano-indentation curves indicated that the saturation shear stress is observed initially at a depth of about 500 nm. At the same time, interface failure is observed experimentally to occur at a greater depth of about 800 nm. However, there is a difference in the stress at which failure occurs, and the post fracture behavior is slightly different. So, the applied stresses are much smaller (since this material is soft) and the amount of elastic energy which is stored in the material before fracture is relatively small. There is no discrete stress drop at the point where the decohesion can be observed to initiate.

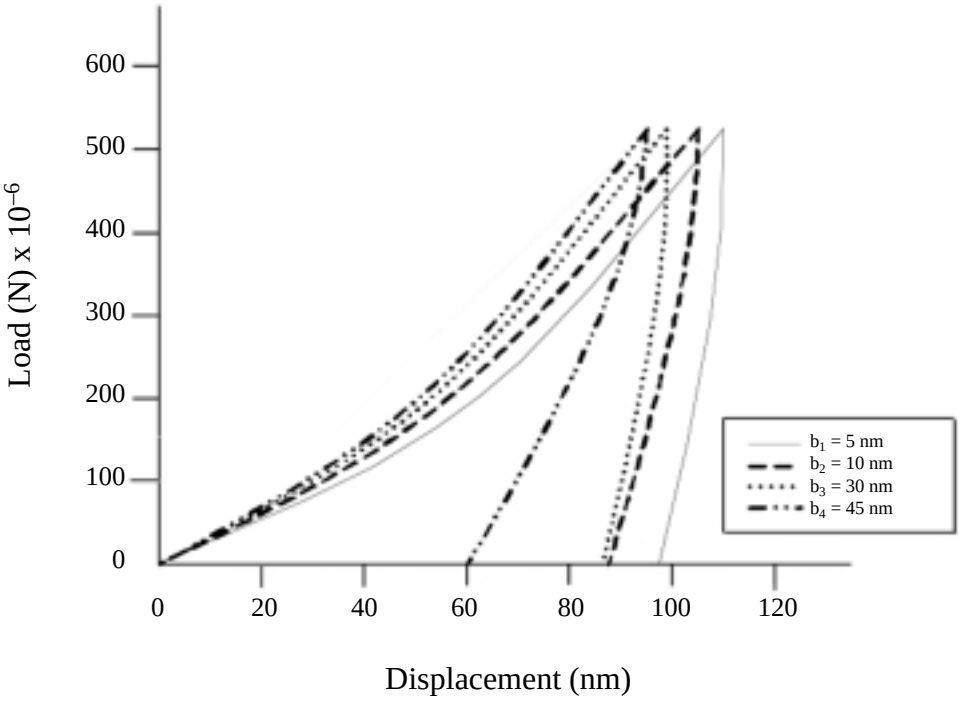

Figure 3. Effect of different coating thickness on articular surface from 5 nm. to 45 nm.

Next, we tested the effect of variation in load-displacement with different coating thickness on articular cartilage from 5 nm to 45 nm. We found that the force displacement response is dependent on the indenter angle, especially at large displacement. Then, a consistent softening response exists with decreasing coating thickness. Thus the effect of the surface hardening is pronounced even at very low levels of deformation as shown in Figure 3. Whereas Figure 4 shows the finite element indentation response as a function of coating thickness for fixed film-substrate Young's modulus ratio with $E_f / E_s = 2$, and different film thickness. The analysis is terminated at a relatively low level of indentation, $\Delta = 80$ nm. The case with layer thickness, b = 10 nm did not converge beyond, $\Delta = 50$ nm, because of a tight applied convergence tolerance.

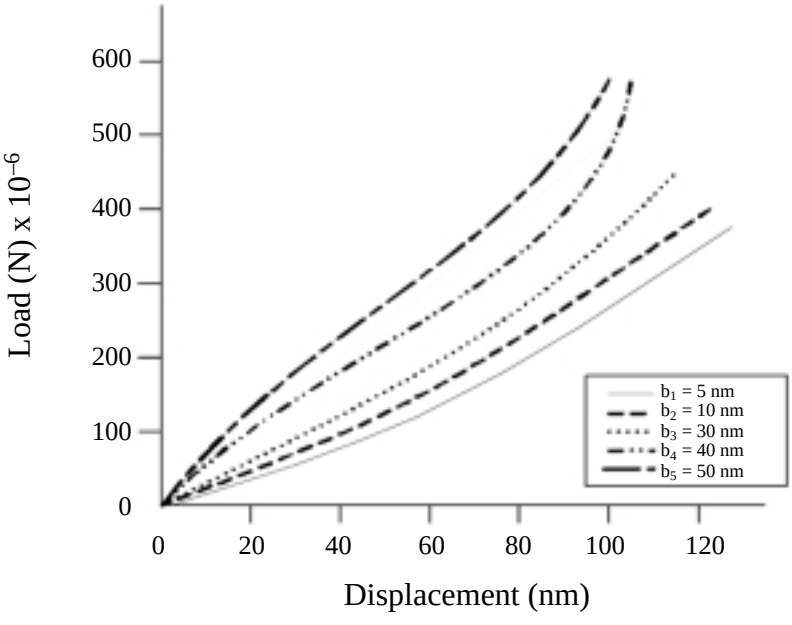

Figure 4. FE indentation response as a function of coating thickness for fixed film-substrate.

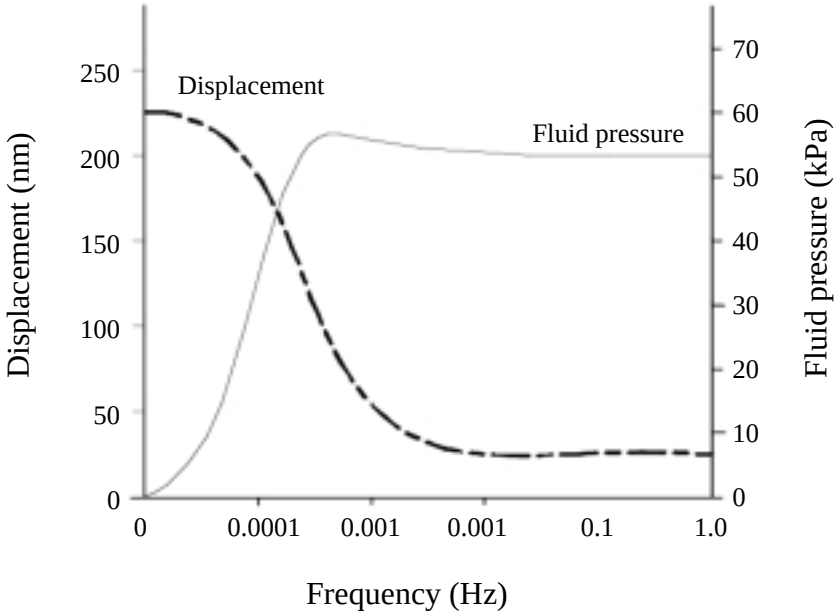

Figure 5. Displacement and fluid pressure responses in nanoindentation cyclical loading as a function of various loading frequency for an axisymmetric model.

Furthermore, we used the Equation (8) and (10) for the test of fluid pressure response when articular cartilage received dynamic loading. Figure 5 shows the observed experimental phenomena on the basis of what is known from theory (Mow et al., 1980; Gu et al., 1998). The interaction between these stress components varies as a function of loading frequency. For very low loading frequencies, $f << f_c$, the tissue rate of deformation is sufficiently slow that interstitial water has ample time to flow in and out of the specimen with negligible drag against the solid matrix. Consequently, the interstitial fluid pressurizes negligibly throughout the depth of the tissue, including at the pressure port interface, and the majority of the applied stress must be supported by the elastic stress in the solid matrix; the deformation of the cartilage plug is then greatest at those lower frequencies and more in phase with the applied stress. Conversely, at high loading frequencies, $f >> f_c$, the rate at which the load is applied greatly exceeds the rate at which the fluid can flow with negligible resistance through the porous permeable matrix. Since fluid must nevertheless flow into and out of the tissue because of the requirement for conversation of mass, a large pressure gradient must build up inside the tissue to overcome the large drag force between the solid and fluid phases.

CONCLUSION

The nanoindentation testing has been applied to a soft, thin high impact articular cartilage coating adhering to a soft substrate. The indenter was a cylindrical, driven at constant displacement rate, normal to the coated cartilage surface. The resultant phenomena of the interface between the coating and substrate were studied experimentally and analyzed, using finite element modeling. Furthermore, this study has found that interstitial fluid pressurization develops at frequencies as low as 10^{-4} Hz, thus, even a loading cycle which take 10^4 sec to complete results in significant interstitial fluid pressurization. It is reasonable to extrapolate these results to physiological conditions in human diarthrodial joints by noting that all activities of daily living involve some amount of motion and deformation, at frequencies in excess of 10^{-4} Hz, even in seemingly-static postures such as standing and sitting, which may have important implications in our understanding of cartilage metabolism and chondrocyte biology under physiological conditions.

REFERENCES

Ateshian, G. A., H. Wang, and W. M. Lai. 1998. The role of interstitial fluid pressurization and surface porosities on the boundary friction of articular cartilage. J. Tribol. 120: 241–251.

Fouvry, S., T. Liskiewicz, Ph. Kapsa, S. Hannel, and E. Sauger. 2003. An energy description of ware mechanisms and its applications to oscillating sliding contacts. Wear 225: 287-298.

Fridrici, V., S. Fouvry, P. Kapsa, and P. Perruchaut. 2003. Impact of contact size and geometry on the lifetime of a solid lubricant. Wear 255: 875–882.

Gray, M. L., A. M. Pizzanelli, A. J. Grodzinsky, and R. C. Lee. 1988. Mechanical and physicochemical determinants of the chondrocyte biosynthetic response. J. of Orthop. Res. 6: 777–792.

Gu, W. L., W. M. Lai, and V. C. Mow. 1998. A mixture theory for charged hydrated soft tissues containing multi-electrolytes: passive transport and swelling behaviors. J. Biomech. Eng. 120: 169–180.

Holmes, M. H., and V. C. Mow. 1990. The non-linear charactevistics of soft gels and hydrated connective tissues in ultrafiltration. J. Biomech. 23: 1145–1156.

Macirowski, T., S. Tepic, and R. W. Mann. 1994. Cartilage stresses in the human hip joint. J. Biomed. Eng. 116:11–18.

Mak, A. F. 1986. Apparent viscoelastic behavior of articular cartilage-The contributions from the intrinsic matrix viscoelasticity. J. Biomech. Eng. 108: 123–130.

Mow, V. C., S. Kuei, W. M. Lai, and C. G. Armstrong. 1980. Biphasic creep and stress relaxation of articular cartilage in compression: theory and experiments. J. of Biomed. Eng. 102: 73–84.

Oloyede, A., and N. D. Broom. 1991. Is classical consolidation theory applicable to articular artilage deformation? Clin. Biomech. 6: 206–212.

Punantapong, B., S. Thongtem, M. J. Fagan, and C. Soorapanth. 2005. Finite deformation behavior of biological soft material on cartilage anisotropy under loading conditions. Proc. of 3rd Int. Conf. on Mat. for Adv. Tech. (ICMAT 2005). 3–8 July 2005, Singapore.

Sah, R. L. Y., Y. J. Kim, J. Y. H. Doong, A. J. Grodzinsky, A. H. K. Places, and J. D. Sandy. 1989. Biosynthetic response of cartilage explants to dynamic compression. J. Orthop. Res. 7: 619–636.

Setton, L. A., W. Zhu, and V. C. Mow. 1993. The biphasic poroviscoelastic behavior of articular cartilage : Role of the surface zone in governing the compressive behavior. J. Biomech. 26: 581–592.

Suh, J. K., Z. Li, and S. L. Y. Woo. 1995. Dynamic behavior of biphasic cartilage model under cyclic compressive loading. J. Biomech. 28: 357–364.

Swadener, J. G., and G. M. Pharr. 2001. Indentation modulus of elasticity anisotropic half-spaces by cones and parabolae of revolution. Philos. Mag. A81: 447–466.

Vlassak, J. J., and W. D. Nix. 1994. Measuring the elastic properties of anisotropic materials by means of indentation experiments. J. Mech. Phys. Solids. 42(8): 1223–1245.